Organic & Biomolecular Chemistry

Cite this: *Org. Biomol. Chem.*, 2011, **9**, 4481

www.rsc.org/obc

PAPER

A dumbbell double nicked duplex dodecamer DNA with a PEG_6 tether†

Karolina Hyz,[a] Wojciech Bocian,[a,b] Robert Kawęcki,[b,c] Elżbieta Bednarek,[b] Jerzy Sitkowski[a,b] and Lech Kozerski*[a,b]

Received 19th January 2011, Accepted 24th March 2011
DOI: 10.1039/c1ob05103b

A hairpin dodecamer DNA motif with a dangling end composed of four bases was studied in order to find conditions which promote a dumbbell structure as the sole form in solution. It could be used as a model of a DNA duplex with two nicks on opposite strands, mimicking a target for topo II poisons. We have established two alternative means of obtaining a dumbbell in solution as the only form present at 0 °C. The first one is to use a relatively high concentration of a hairpin motif, *ca.* 3.5 mM, at low ionic strength, and second is to use a moderate hairpin motif concentration of *ca.* 2 mM at high ionic strength, 200 mM and 15% of methanol. An NMR-derived structure in a buffered water solution is presented. A representative structure ensemble of 10 structures was obtained from MD calculations utilizing the AMBER protocol and using NOESY-derived experiment cross peak volumes transferred to experimental restraints by the MARDIGRAS algorithm.

Introduction

There is continuing interest in new classes of compounds find leads and better formulations of anticancer drug pharmacophores.[1,2,3,4,5] Topoisomerase I, II (topo I, II) poisons attract much attention in biomedical research in this direction since they constitute an important chemotherapeutic route for combating cancer.[6,7,8]

Topoisomerases are essential enzymes that relieve the torsion stress produced in DNA during replication by cutting DNA on one strand, allowing the broken strand to rotate around the uncut strand.[9,10] Two nicks, one in each strand, which are separated by four base-pairs, are generated by topo II,[11] which plays several roles in cell life.[12]

We have recently shown that a nicked decamer DNA duplex with a PEG_6 tether[13] is a useful model for studying the secondary complex with topo I poison, TPT, by solution NMR.[14] Not only did we prove the DNA/TPT geometry found in X-ray structure of the ternary complex of topo I/TPT/nicked DNA,[15] but we were also able to address the questions left unanswered by the X-ray study.

Our interest in dumbbell nicked DNA is related to the problem of targeting the secondary complex with topo II by genistein,[7] since the mechanism of its action on an atomic level in this complex is not known.[16] The structure of the dumbbell DNA duplex to be used in this study, as a component of the ternary complex topo II/nicked DNA/genistein, is shown in Scheme 1.

Scheme 1 Double nicked dumbbell DNA.

The choice of nucleotides around the nick was based on the result of a biological assay that disclosed that genistein is the organic ligand showing thymine requirements at both positions –1 and +1.[7]

The problem of a nicked DNA model relevant to topo II is inherently connected with the hairpin motifs of the DNA oligomers.[17,18] A few spectroscopic studies of oligonucleotides with non-nucleotide bridges have been performed.[19,20] Some generalizations concerning the hairpin–duplex equilibrium were established earlier.[21] In general, the hairpin form is favored at both low salt and hairpin concentration. More importantly, the dynamics and position of the equilibrium depend strongly on the base-pair sequence, and particularly on a dimer interface that comprises only four base-pairs.

Our main goal in this study was to optimize the conditions under which the dumbbell forms in solution as the sole form, as a model to study interactions with topo II poisons. After these conditions had been found, we established its structure by NMR.

[a]*Institute of Organic Chemistry, Polish Academy of Sciences, Kasprzaka 44, 01-224, Warszawa, Poland. E-mail: lkoz@icho.edu.pl; Fax: +48 22 632 6681; Tel: +48 22 343 2018*

[b]*National Medicines Institute, Chełmska 30/34, 00-725, Warszawa, Poland*

[c]*University of Natural Sciences and Humanities, 3. Maja 54, 80-110, Siedlce, Poland*

† Electronic supplementary information (ESI) available: ^{1}H NMR and NOESY spectra, chemical shifts of hairpin and dumbbell motifs, averaged global parameters of ten computed structures of a dumbbell. See DOI: 10.1039/c1ob05103b

Results and discussion

Ionic strength, hairpin concentration and organic cosolvent influence on the hairpin–dumbbell equilibrium

Scheme 2 shows the hairpin–dumbbell equilibrium, the subject of this study. There are two prerequisite conditions which should be fulfilled in order that the dumbbell can serve as a good model for studying topo II poisons. The concentration of the hairpin should be as low as possible because the DNA oligomers tend to aggregate in water at lower temperatures, which makes it difficult to run NMR experiments based on scalar coupling, since the signals are getting broader. On the other hand, it should be possible to saturate the solution with organic ligands (topo II poisons) that are usually hardly soluble in water, and therefore the salt concentration cannot be too high to avoid salting out the organic ligand.

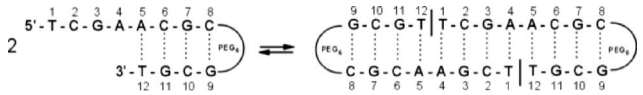

Scheme 2 The hairpin–dumbbell equilibrium.

Introducing G–C base-pairs in the dimer interface, expecting to strengthen duplex formation, cannot be applied in the present model, because genistein binding in the nicks requires thymidines at both −1 and +1 positions.

We have therefore studied the concentration dependence of the solute, and also the solvent (Fig. 1) ionic strength influence, on the position of the equilibrium in order to find the conditions that will promote dumbbell formation at moderate solute concentration, *ca.* 1–2 mM hairpin, and would give sharp signals allowing NMR experiments based on scalar coupling to be run.

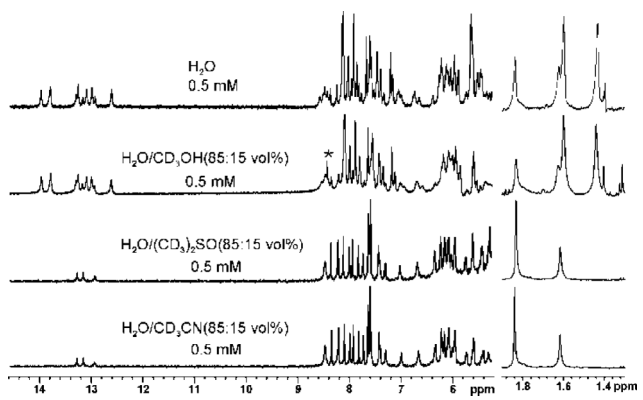

Fig. 1 Organic solvent dependence of the hairpin–dumbbell equilibrium in a 25/25 mM K_3PO_4/NaCl buffer at 0 °C. The thymidine resonances are displayed on the right-hand side of the spectra . The low frequency signals at 1.44 and 1.60 ppm are characteristic of a dumbbell structure.

A classical approach to increase the dumbbell population by raising the ionic strength does not work sufficiently well at low solute concentration in the present case (*ca.* 0.5 mM of hairpin, Fig. 1S, ESI†). Raising the hairpin concentration to over 2 mM allows a shift of the equilibrium towards the dumbbell at 0 °C (Fig. 2S, ESI†).

Likewise, raising the ionic strength to 200 mM of NaCl at this concentration promotes the dumbbell structure at this temperature (Fig. 2 and Fig. 2S, ESI†).

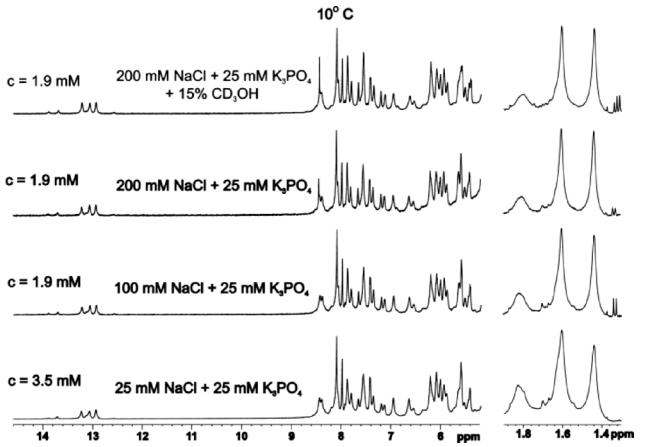

Fig. 2 The ionic strength influence on the equilibrium at high DNA hairpin concentration.

The spectral results of the organic solvent influence on the studied equilibrium are summarized in Fig. 1, which shows diagnostic spectral regions of thymidine methyl and imine resonances. At 0 °C in neat water (upper spectrum), two sets of thymidine signals are displayed, at 1.83 and 1.63 ppm, assigned to the hairpin motif, and at 1.44 and 1.60 ppm, assigned to the dumbbell. Ten NH resonances at 12.5–14 ppm are seen, six of which, of higher intensity, are assigned to the dumbbell structure. At 0 °C in pure water, as shown in Fig. 1, there is *ca.* 50 mol% dumbbell present, characterized by thymidine chemical shifts at 1.60 and 1.44 ppm. This assignment is based on the fact that a low frequency shift is observed for both methyl groups that is characteristic of base-pairing, as compared to the hairpin motif. Furthermore, this set of signals enhances in intensity with lowering of the temperature, as seen in Fig. 3S, ESI.† The site specific assignment for each methyl group is established by a NOESY spectrum. There are clearly seen two sets of overlapping signals due to the hairpin and dumbbell motifs at an intermediate exchange rate, indicated by broadening of the signals. The addition of 15 vol% of methanol changes the equilibrium of both species in favor of the dumbbell form, which is present in *ca.* 60 mol% population. Even at this low concentration of solute, the signals are quite broad. Further lowering the temperature to below 0 °C does not result in any significant line sharpening, the expected result of a slowing exchange rate. Apparently, aggregation of the dumbbell species cannot be avoided in both solvents, on one hand, and molecular tumbling slows down at this temperature, leading to dipolar broadening.

Quite a different situation is encountered with the 15% addition of aprotic solvents DMSO-d_6 and CD_3CN, with lower dielectric constants than water. There is only one set of signals assigned to the hairpin motif and the signals are much sharper, evidencing a lack of exchange between the two motifs at low temperature. Furthermore, the appearance of NH resonances at 13 ppm confirms the duplex formation in a hairpin. (see Scheme 2) In effect, both solvents prevent dimerization but allow intramolecular hydrogen bond formation. We have recently observed a similar effect of acetonitrile on human insulin aggregation in H_2O/CD_3CN (65 : 35 vol%); it disrupts the quaternary structure of the protein but leaves the tertiary structure intact, thus allowing monomer structure elucidation at an NMR-accessible concentration.[22]

Fig. 2 shows the ionic strength and solute concentration dependence on the hairpin–dumbbell equilibrium. An increased buffer concentration allows the use of a lower dodecamer concentration and the addition of 15% methanol enables sharper lines to be observed and secures a better solubility at lower temperatures of poorly soluble aromatic topo II inhibitors. It is worth noting that the broad signal in the top spectrum at 1.8 ppm is assigned to H2′ of a ribose in cytidine C6 (see Table 2S, ESI†).

In effect, we have established two alternative means of obtaining the dumbbell in solution at 0 °C as the only form present. The first one is to use a relatively high concentration of the hairpin motif, *ca.* 3.5 mM, at low ionic strength, 25 mM, and second, is to use a moderate hairpin motif concentration, *ca.* 2 mM, at a high ionic strength, 200 mM NaCl and 15% methanol.

The hairpin structure at 25 °C

In view of the above findings on the factors affecting the equilibrium, we decided to assign first the resonances characteristic for the hairpin in water at pH 6, and the low buffer and solute concentrations at ambient temperature to assure the conditions close to physiological and with no exchange with the dumbbell.

Fig. 3S, ESI† shows the temperature dependence of the hairpin–dumbbell equilibrium in 0.35 mM DNA in water in a 25/25mM K_3PO_4/NaCl buffered solution. At 0 °C, both forms are in a slow exchange regime of the hairpin–dumbbell equilibrium. This is evidenced by the nearly identical half-width of the signals, despite the fact that both forms are in unequal populations in equilibrium. Nevertheless, this spectrum is not amenable to structural investigation due to overlap of the signals belonging to the two species in solution.

At 10 °C, both forms are in an intermediate exchange limit on the NMR time-scale. At 25 °C, only one set of thymidine methyl signals is observed. This set of signals is assigned to the hairpin structure (Scheme 2). More important is a fact that no signal at 1.43 ppm is seen, which can be taken as evidence that no dimer is present in solution at this concentration and temperature. We have therefore characterized the chemical shifts of the hairpin motif at 25 °C.

The presence of NH resonances in the 13 ppm region in the spectrum at 25° C confirms the existence of a duplex in the hairpin motif (Table 1S, ESI†) and in the dumbbell (see Table 2S and Fig. 4S, ESI†). The guanosine NH resonances in the hairpin motif were assigned to G11, G7 and G9 at 12.87, 13.10 and 13.22 ppm, respectively, in agreement with the increasing hydrogen bond strength due to the longer distance from the dangling motif. The NHs of G3, T1 and T12 are not observed in the spectrum of the hairpin motif as they are broad and fast exchanging with water. On the other hand, in a spectrum at 0 °C, all six resonances are observed, giving evidence of a duplex structure at the dimer interface region. The linear single strand structure of the hairpin motif can be rejected on the discussed basis.

The fingerprint region of the hairpin motif in a NOESY spectrum is shown in Fig. 3. Projections in Fig. 3 show that some signals in both traces are broader than others. The broader signals characterize the dangling end that does not have a duplex structure, and therefore has a much higher mobility. In general, the crosspeaks are weak. Table 1S, ESI† comprises the chemical shifts of the protons in the nucleotide units in the DNA hairpin motif at 25 °C.

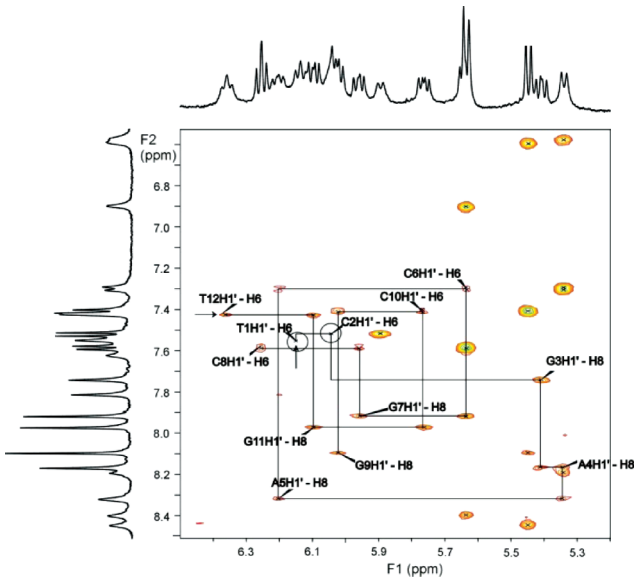

Fig. 3 Fingerprint region of the NOESY spectrum of hairpin DNA at 25 °C, 0.35 mM, pH 6.1 in 25/25 mM K_3PO_4/NaCl water buffer.

The dumbbell motif assignments and structure calculation

In order to observe the dumbbell structure as the sole form (Scheme 1) in neat water, we raised the hairpin concentration to 3.5 mM in the monomer and a low buffer concentration was used to avoid salting out the expected dimer at 0 °C. This is illustrated in the bottom spectrum in Fig. 2 at 10 °C (compare also Fig. 2S, ESI† at 0 °C).

We undertook an attempt to calculate the structure of the dumbbell on the basis of NOESY cross peaks at 0 °C. Fig. 4 shows that the ^{1}H NMR spectrum is quite broad, and only a NOESY

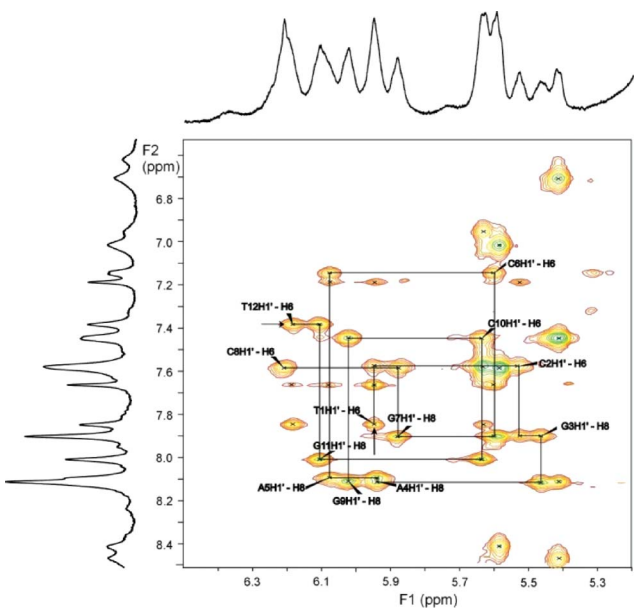

Fig. 4 Fingerprint region of the NOESY spectrum of dumbbell DNA at 0 °C, 3.5 mM monomer, pH 6.1 in 25/25 mM K_3PO_4/NaCl buffer.

Table 1 Statistical parameters for an ensemble of 10 computed structures of dumbbell DNA motifs with two nicks in opposite strands

Total no. of NOE restraints	431
Inter-strand	37
Watson–Crick restraints	52
Numbers of structures calculated	10
All atom rmsd	0.79 ± 0.12
Average restraint violation energy	210 kcal mol^{-1}
Average number of distance violations > 0.2 Å < 0.3 Å	23
Average number of distance violations > 0.4 Å < 0.4 Å	2

spectrum could be acquired as a source of spectral assignments and experimental restraints. TOCSY and HSQC experiments, useful for ribose proton assignment, were not available due to the large half-width of the signals. All the important interstrand NOEs were observed (see Fig. 4S, ESI†), which are crucial for structure assignment. Some spectral features are worth mentioning with respect to the tertiary structure of the dumbbell. First, Fig. 4S, ESI† shows that the NH of G3 resonates at the lowest frequency of all four G units and the signal is slightly broader than the others. This is derived from the fact that G3 is in a dimer interface, which can have a higher mobility and therefore the hydrogen bond to C2 is weaker. Secondly, on the other hand, the thymidine NHs are narrow and displaced at the highest frequencies, giving support to a reasoning that the dimer structure is fairly rigid and the nicks are well defined. Nevertheless, it was possible to extract enough NOESY cross peak volumes to effectively run MD calculations (see the Experimental for details).

Table 1 gives the statistics for 10 computed structures of the studied dumbbell motif with two nicks in opposite strands.

Fig. 5 shows an ensemble of 10 computed structures of the dumbbell double nicked DNA dodecamer calculated using the Generalized Born (GB) protocol for the solvent. An examination of base-pairs and inter-base parameters (Tables 3S–6S, ESI†) confirms a regular B-DNA structure. The differences of individual parameters compared to the canonical form were computed. The largest changes are plotted in Fig. 5S, ESI† concerning the inclination (η°) and tip (Θ°) parameters. Fig. 5S, ESI† shows that these parameters do not differ from the canonical form in the dimer interface but are large close to the PEG_6 linker. This is intuitively expected as the linker introduces a non-natural rigidity but the motifs around the nick well reproduce the canonical form. Furthermore, the 5′-CH_2OH and 3′-PO_3 groups at the nick point are outside the molecule surface and therefore their conformation should not be relevant to topo II poison binding.

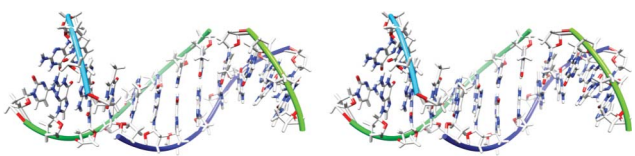

Fig. 5 A stereo view average of 10 computed structures of the dumbbell 12-dodecamer double nicked DNA after the simulating annealing protocol. The PEG_6 linker is omitted.

In order to check the natural propensity of the hairpin motif to dimerize, we performed the MD calculation without constraints on the final step of the structure refinement in a water box. The result is presented in Fig. 6.

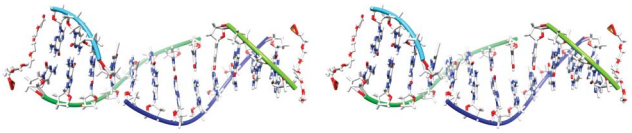

Fig. 6 A stereo view average of 10 computed structures of the dumbbell 12-dodecamer double nicked DNA after molecular dynamics without constraints.

Molecular dynamics calculations showed that the hairpin motif has an intrinsic desire to dimerize, and the dynamics of the dimer are essentially unchanged with respect to that obtained after the simulated annealing structure refinement protocol (see Tables 7S and 8S, ESI†). Some structural distortions were observed that could be accounted for by the force field used (*ff*99SB).

Experimental

The hairpin DNA was purchased from IDT as a 5′-TCGAACGC/iSp18/GCTG/3Phos/-3′ dodecamer with a PEG_6 linker (iSp18). The oligonucleotide was purified by ion-exchange chromatography on a HiTrap™-Q column (Pharmacia Biotech) using gradient elution with an ammonium bicarbonate solution (0.1–0.8 M) and de-salted on a Sephadex G-10 filled column.

Sample preparation

Samples for NMR were prepared by dissolving the oligonucleotide in buffer containing 25 mM K_3PO_4 and a variable amount of sodium chloride (25–200 mM) to study the ionic strength dependence on the hairpin–dumbbell equilibrium. The pH was adjusted to 6.0 or higher. Samples in H_2O contained 10 vol% D_2O. The concentration was measured by UV absorption. TSP-d_4 was added to monitor the changes of chemical shifts at different temperatures. No EDTA was added to the samples, which were purified to remove paramagnetic impurities on a Chelex 100 column packing purchased from Bio-Rad Laboratories.

NMR experiments

500 and 600 MHz ^{1}H NMR spectra in H_2O on Varian NMR spectrometers were run in a 12 or 16 kHz spectral window, respectively, using the WATERGATE sequence[23] for water suppression for samples in H_2O (1–2 ms soft pulses).

NOESY spectra[24] (DPFGSE_NOESY), with water suppression by gradient echo and ZQ artifact suppression during mixing, were recorded using the States-TPPI method[25,26] (mixing time 150 ms). Typically, 2048 × 512 data points with 64 transients each and a recycle delay of 2 s were collected in f2 and f1. Prior to FT, data were zero-filled to give a 4 K × 4 K matrix, and both dimensions were apodised with shifted squared sine bell functions.

Calculation procedures

The 374 NOE cross peak volumes were assigned from the NOESY spectra at a 150 ms mixing time using SPARKY[27] for the assignment of cross peaks and the integration of their volumes. The NOE volumes were converted to upper and lower bound restraints using MARDIGRAS (v. 5.21).[28,29] The MARDIGRASS algorithm converts the intensity matrix (non-observable intensities are supplied from the model) to a relaxation rate matrix, which is

improved by an iterative procedure. Distances are then calculated from the final cross relaxation rates. This yielded 431 restraints, considering the *C*2 symmetry of the molecule. MD refinement in AMBER 9[30] involved additionally 52 Watson–Crick restraints. The GB solvent model[31,32] approach was used in the refinement protocol using molecular dynamics simulated annealing.

Refinement protocol

The 500 energy minimization with the GB model was first performed on 10 starting dumbbell molecules built using A and B DNA type canonical structures and intermediates. This was followed by two cycles of 15 ps simulated annealing with GB performed by *SANDER* (from AMBER): 0–1000 steps heating the system from 10 to 1100 K, 1001–3000 steps leaving at 1100 K, 3000–15000 steps cooling to 0 K, 0–3000 steps tight coupling for heating and equilibration (TAUTP = 0.2), 3001–11000 steps of slow cooling (TAUTP = 4.0–2.0), 11000–13000 steps of faster cooling (TAUTP = 1.0) and 13000–15000 steps of fast cooling, like a minimization (TAUTP = 0.5–0.05), in steps 0–3000 the restraints were slowly increased from 10 to 100% of their final values. A cutoff value was set at 15 Å.

Molecular dynamics

For 10 structures after simulated annealing, 40 ns molecular dynamics in a water box was run. 10 ps snapshots were saved and finally averaged to yield a final 10 structures.

The particle mesh Ewald (PME) method was used to treat long-range electrostatic interactions with a cubic B-spline interpolation and a 10^{-5} tolerance for the direct space sum cutoff. A 9 Å cutoff was applied to non-bonded Lennard–Jones interactions. The SHAKE algorithm was applied to constrain all bonds involving hydrogen atoms with a tolerance of 10^{-5} Å^2, and a 2 fs time step was used in the dynamics simulation. All systems used the same minimization and equilibration protocols. First, the water molecules and counterions were minimized for 1000 steps of steepest descent and 4000 of the conjugate gradient method with the DNA restrained by 10 kcal mol^{-1} Å^{-2} to their initial positions, followed by a second unrestrained minimization. The next steps of the equilibration protocol were 15 ps constant volume dynamics MD with 5 kcal mol^{-1} Å^{-2} restraints on the DNA and topotecan, with the system gradually heated from 10 to 300 K using the Berendsen coupling algorithm with a coupling parameter of 1 ps. Then, using a 50 ps constant pressure MD with a 1 ps pressure relaxation time, the density of the system was adjusted close to 1 g cm^{-3}. During a subsequent 35 ps of constant volume and temperature dynamics, the restraints on the DNA base-pairs were gradually reduced to 0 kcal mol^{-1} Å^{-2}.

Conclusions

A hairpin DNA duplex with a PEG_6 linker on the 5′-3′ ends of complementary strands and with four bases at the dangling end was studied in order to establish the conditions for the observation of a dumbbell motif as the sole form in solution. This form is expected to mimic the target for topo II poisons.

We have established two alternative means of obtaining the dumbbell as the sole form in solution at 0 °C (Fig. 2S, ESI†). The first one is to use a relatively high concentration of the hairpin motif, *ca.* 3.5 mM, at low ionic strength, 25 mM NaCl, and the second is to use a moderate hairpin motif concentration, *ca.* 2 mM, at high ionic strength, 200 mM and 15% methanol. The dumbbell structure, based on MD calculations using experimental NOE restraints, is presented. MD calculations performed in a water box without restraints showed essentially the same structure.

Acknowledgements

The authors acknowledge financial support during this research from the Ministry of Science and Higher Education Grant no. N N204 155736.

References

1 P. B. Arimondo, G. S. Laco, C. J. Thomas, L. Halby, D. Pez, P. Schmitt, A. Boutorine, T. Garestier, Y. Pommier, S. M. Hecht, J. S. Sun and C. Bailly, *Biochemistry*, 2005, **44**, 4171–4180.
2 K. Cheng, N. J. Rahier, B. M. Eisenhauer, R. Gao, S. J. Thomas and S. M. Hecht, *J. Am. Chem. Soc.*, 2005, **127**, 838–839.
3 N. J. Rahier, B. M. Eisenhauer, R. Gao, S. H. Jones and S. M. Hecht, *Org. Lett.*, 2004, **6**, 321–324.
4 A. Cagir, S. H. Jones, R. Gao, B. M. Eisenhauer and S. M. Hecht, *J. Am. Chem. Soc.*, 2003, **125**, 13628–13629.
5 P. Pourquier and Y. Pommier, *Adv. Cancer Res.*, 2001, **80**, 189–216.
6 M. Palumbo, B. Gatto, C. Sissi, in *DNA and RNA Binders, From Small Molecules to Drugs*, ed. B. C. Demeunynck and W. D. Wilson, Wiley, New York, 2002, pp. 503–537.
7 G. Capranico, M. Palumbo, S. Tinelli, M. Mabilia, A. Pozzan and F. Zunino, *J. Mol. Biol.*, 1994, **235**, 1218–1230.
8 H. K. Wang, S. L. Morris-Natschke and K. H. Lee, *Med. Res. Rev.*, 1997, **17**, 367–425.
9 J. C. Wang, *Annu. Rev. Biochem.*, 1996, **65**, 635–692.
10 L. Stewart, M. R. Redinbo, X. Y. Qiu, W. G. J. Hol and J. J. Champoux, *Science*, 1998, **279**, 1534–1541.
11 J. M. Berger, S. J. Gamblin, S. C. Harrison and J. C. Wang, *Nature*, 1996, **379**, 225–232.
12 A. K. Larsen, A. E. Escargueil and A. Skladanowski, *Prog. Cell Cycle Res.*, 2003, **5**, 295–300.
13 L. Kozerski, A. P. Mazurek, R. Kawęcki, W. Bocian, P. Krajewski, E. Bednarek, J. Sitkowski, M. P. Williamson, A. J. Moir and P. E. Hansen, *Nucleic Acids Res.*, 2001, **29**, 1132–1143.
14 W. Bocian, R. Kawęcki, E. Bednarek, J. Sitkowski, M. P. Williamson, P. E. Hansen and L. Kozerski, *Chem.–Eur. J.*, 2008, **14**, 2788–2794.
15 B. L. Staker, K. Hjerrild, M. D. Feese, C. A. Behnke, A. B. Burgin, Jr. and L. Stewart, *Proc. Natl. Acad. Sci. U. S. A.*, 2002, **99**, 15387–15392.
16 W. Bocian, R. Kawęcki, E. Bednarek, J. Sitkowski, A. Ulkowska and L. Kozerski, *New J. Chem.*, 2006, **30**, 467–472.
17 S. Singh, P. K. Patel and R. V. Hosur, *Biochemistry*, 1997, **36**, 13214–13222.
18 E. A. Snowden-Ifft and D. E. Wemmer, *Biochemistry*, 1990, **29**, 6017–6025.
19 M. Durand, K. Chevrie, M. Chassignol, N. T. Thuong and J. C. Maurizot, *Nucleic Acids Res.*, 1990, **18**, 6353–6359.
20 H. Gao, N. Chidambaram, B. C. Chen, D. E. Pelham, R. Patel, M. Yang, L. Zhou, A. Cook and J. S. Cohen, *Bioconjugate Chem.*, 1994, **5**, 445–453.
21 F. J. Van de Ven and C. W. Hilbers, *Eur. J. Biochem.*, 1988, **178**, 1–38.
22 W. Bocian, J. Sitkowski, E. Bednarek, A. Tarnowska, R. Kawęcki and L. Kozerski, *J. Biomol. NMR*, 2008, **40**, 55–64.
23 M. Piotto, V. Saudek and V. Sklenar, *J. Biomol. NMR*, 1992, **2**, 661–665.
24 J. Jeener, B. H. Meier, P. Bachmann and R. R. Ernst, *J. Chem. Phys.*, 1979, **71**, 4546–4553.
25 G. Bodenhausen, H. Kogler and R. R. Ernst, *J. Magn. Reson.*, 1984, **58**, 370–388.
26 D. J. States, R. A. Haberkorn and D. J. Ruben, *J. Magn. Reson.*, 1982, **48**, 286–292.
27 T. D. Goddard and D. N. Kneller, *SPARKY*, University of California, San Francisco.

28 B. A. Borgias and T. L. James, *Methods Enzymol.*, 1989, **176**, 169–183.
29 T. L. James, B. A. Borgias, A. M. Bianucci and N. Zhou, *Basic Life Sci.*, 1990, **56**, 135–154.
30 D. A. Case, T. A. Darden, T. E. Cheatham III, C. L. Simmerling, J. Wang, R. E. Duke, R. Luo, K. M. Merz, D. A. Pearlman, M. Crowley, R. C. Walker, W. Zhang, B. Wang, S. Hayik, A. Roitberg, G. Seabra, K. F. Wong, F. Paesani, X. Wu, S. Brozell, V. Tsui, H. Gohlke, L. Yang, C. Tan, J. Mongan, V. Hornak, G. Cui, P. Beroza, D. H. Mathews, C. Schafmeister, W. S. Ross and P. A. Kollman, *AMBER 9*, University of California, San Francisco, 2006.
31 A. Onufriev, D. Bashford and D. A. Case, *J. Phys. Chem. B*, 2000, **104**, 3712–3720.
32 B. Xia, V. Tsui, D. A. Case, H. J. Dyson and P. E. Wright, *J. Biomol. NMR*, 2002, **22**, 317–331.

